Mineralogy, Geochemistry and Stable Isotope Investigation of Gürkuyu Sb Mineralization (Gediz-Kütahya-NW Turkey)

Yeşim ÖZEN, Fetullah ARIK

Department of Geological Engineering, Selçuk University, 42079 Konya, Turkey

Abstract. The Gürkuyu Sb mineralization is located in the western part of Anatolian tectonic belt, in southern part of İzmir-Ankara zone and in northern part of Menderes Massif. The mineralization located at west of the Koca hill in east of Gürkuyu village of Gediz (Kütahya-Turkey) has been characterized through the detailed examinations involving sulfur and oxygen isotope. Serpentinites of Dağardı melange and crystallized limestones of Budağan limestone were hydrothermally altered by hydrothermal solutions, come from fissures and fractures due to tectonic movement during the thrust of melange and occurred silicified zone. Gürkuyu Sb mineralization suggest that occurred in this silicified zone. In Gürkuyu mineralization, primary ore minerals are antimonite and pyrite, secondary ore minerals are senarmontite, valentinite, orpiment and realgar. Quartz and calcite are the most common gangue minerals. In mineralization, average contents of Fe_2O_3, Sb, Hg, As and Au are 2.15 wt.%, 13359 pm, 1.12 ppm, 1367 ppm and 163.82 ppb, respectively. In Gürkuyu Sb mineralization, $\delta^{34}S$ values of stibnite are ranged from 1.0 ‰ to 1.3 ‰. $\delta^{18}O$ values of quartz are ranged is 15.8 ‰ in Gürkuyu mineralization. Sulfur and oxygen isotope values are similar to the values for magmatic rocks and to the values for fluids of magmatic origin.

Keywords: stable isotope, Gürkuyu, Sb mineralization, Gediz, Kütahya, NW Turkey.

Gürkuyu Sb Cevherleşmesinde (Gediz Kütahya Türkiye) Mineraoloji, Jeokimya ve Kararlı İzotop İncelenmesi

Özet. Gürkuyu Sb cevherleşmesi Anadolu tektonik kuşağının batısında, İzmir-Ankara zonunun güneyinde, Menderes Masifinin kuzeyinde yer almaktadır. Koca Tepe batısında, Gürkuyu Köyü (Gediz (Kütahya) güneyinde yer alan cevherleşmede mineraloji, jeokimya ve duraylı izotop (S,O) çalışmaları yapılmıştır. Dağardı melanjının bindirmesi esnasında ve daha sonra devam eden tektonik hareketlere bağlı olarak oluşan kırık ve çatlaklardan gelen hidrotermal çözeltilerin, Dağardı melanjına ait serpantinitlerle Budağan kireçtaşlarına ait kristalize kireçtaşlarını hidrotermal alterasyona uğratarak oluşan silisleşmiş zon içinde Gürkuyu antimonit cevherleşmesini meydana getirdiği düşünülmektedir. Gürkuyu cevherleşmesinde birincil cevher mineralleri antimonit ve pirit iken ikincil cevher mineralleri senarmontit, valentinit, orpiment ve realgardır. Kuvars ve kalsit ise en yaygın gang mineralleridir. Cevherleşmede Fe_2O_3, Sb, Hg, As ve Au değerleri sırasıyla % 2.15, 13359 pm, 1.12 ppm, 1367 ppm ve 163.82 ppb'dir. Gürkuyu Sb cevherleşmesinde antimonitin $\delta^{34}S$ değerleri ‰ 1.0 ile ‰ 1.3 arasında değişmektedir. Kuvarsın $\delta^{18}O$ değeri ise ‰ 15.8'dir. Sülfür ve oksijen izotop sonuçları magmatik kökenli sıvılar ve magmatik kayaçlardaki değerler ile benzerlik göstermektedir.

Anahtar Kelimeler: duraylı izotop, Gürkuyu, Sb cevherleşmesi, Gediz, Kütahya, KB Türkiye

1. INTRODUCTION

Western Anatolia is known as an economically important metallogenic province in the Alpine–Himalayan Belt. The Tethyan Eurasian Metallogenic Belt (TEMB; [1]) extending from Western Europe through Anatolia to Iran is one of the world's major metal producing belts hosting many volcanogenic massive sulfide, porphyry-type (copper–gold and copper–molybdenum), low- and high-sulfidation epithermal (gold and gold–silver), mesothermal (lead, zinc, copper), and skarn (iron– copper, lead–

_____

zinc)-type deposits. The TEMB formed because of the convergence and collision of the Indian, Arabian and African tectonic plates with the Eurasian tectonic plate [2]. Mineral deposits in the northwestern Turkey show similarities, in many ways, with the characteristics of mineral deposits found throughout the TEMB. The mineralization events in western Anatolia have temporal and spatial association with episodic magmatism since the Middle Eocene to Late Miocene–Pliocene [3].

The field observations supported by geochronological and geochemical data [4] on magmatic events suggested that Aegean subduction is accompanied by a lithospheric extension, exhumation, core-complex development, subduction and extension-related magmatism and large-scale, probably gravitational gliding of the Lycian Nappes system approximately between 24 – 23 Ma to Plio-Quaternary [4-8].

Recent work on the tectonic setting and geochronology of magmatic and hydrothermal events within western Anatolia suggested that the mineralization has been an integral part of the closure of the NeoTethys since the Late Cretaceous [3,9,10] and is related to (1) the northward subduction and closure of the marginal Vardar–Izmir–Ankara ocean that was followed by Early–Middle Eocene post collisional magmatism to the north and south of the Izmir–Ankara–Erzincan suture zone (IAESZ), and (2) subduction of the remnant of the NeoTethys oceanic plate along Aegean–Cyprean Arc [3]. The closure of the NeoTethys was followed by extensive extensional regime that produced voluminous calc-alkaline to alkaline, even ultrapotassic magmatism, starting from about Late Oligocene [3].

The Gürkuyu Sb mineralization is located at western part of the Anatolian tectonic belt, in southern part of the İzmir-Ankara zone, and in northern part of the Menderes Massive and part of the Inner West Anatolian of the Aegean Region. The Gürkuyu Sb mineralization is located about 25 km southeast of the Simav (Kütahya-Turkey) and 16 km southwest of the Gediz (Kütahya-Turkey) (Fig. 1).

Several mineralizations (İnkaya Cu-Pb-Zn-(Ag), Değirmenciler Sb, Arpaçukuru Fe-Cu, Pınarbaşı Fe-Cu-Pb-Zn mineralizations, etc.) as well as Gürkuyu Sb mineralization occur along the Simav Graben and were formed in association with a tectono-magmatic period [11-18].

The present study was carried out to investigate the chemical-physical conditions of the hydrothermal fluids and the mechanism of mineralization by using isotopic data. Furthermore, our new data may provide constrains on origin of the mineralizing fluids and the formation mechanism of the Gürkuyu Sb mineralization by using S and O isotopic data.

2. GEOLOGICAL SETTINGS

2.1. Regional geological setting

In western Turkey, recent research has revealed that the extensional regime has been in place since the Late Oligocene-Early Miocene, following earlier collisional events [19]. However, some researchers suggest that the compressional period lasted until the end of the Middle Miocene events [20-23]. The extensional tectonic regime caused the development of metamorphic core complexes, fault-controlled NE- and E-W-trending basins and the emplacement of the magmatic rocks in western Turkey [20, 24-29]. Western Anatolia is a part of the Aegean extensional province (e.g., [30]). Extension in western Anatolia has been attributed to several tectonic causes. The region contains geological features related to geodynamic processes, such as arc-continent collision (e.g., [31]), two-stage basin formation and rift-mode extension ([32]), slab break-off (e.g., [33]), crustal thickening (e.g., [34]), orogenic collapse resulting in core complex formation (e.g., [28,35-37]), a retreating subduction zone (e.g., [38]) and velocity differences between the overriding Aegean and Anatolian plates [39] throughout Cenozoic times. Radiometric dating of syn-tectonic granitoids and detachment-related fault rocks indicate that the

central Menderes, Kazdağ and Simav metamorphic core complexes formed during the Early and Middle Miocene [40,41].

Metamorphic massifs formed the crystalline basement widely distributed and include massifs such as Istranca and Kazdağ Massifs in NW Turkey, Menderes Massif in western Turkey, Kırşehir Massif in central Turkey, and Bitlis Massif in SE Turkey ([42,43], Fig. 2).

In western Turkey, the Pontides and the Anatolide-Tauride Block are separated by an ophiolitic belt, known as the Izmir-Ankara suture zone, thrust southwards onto the Anatolides and Taurides ([31]; Fig 2). After the closure of the N-dipping subduction zone between the Pontides to the NNW and the Anatolide-Tauride platform to the SSE (Late Paleocene to Early Eocene), the İzmir-Ankara suture zone was formed ([31,44])

Granites occur in different tectonic belts in Anatolia, and can be used to understand the geochemical and tectonic evolution of subduction and collision over the past ~ 600 million years. The Late Paleozoic magmatism is an important event in northwest Anatolia [45].

The Gürkuyu Sb mineralization is located at the boundary between Menderes Massif and Afyon tectonic zone with several NNW-trending active fault zones in NW Turkey (Fig. 2). The region is within the Anatolides tectonic unit and west of the Kırşehir Block (Fig. 2). The Anatolides consist of the Tavşanlı zone, the Afyon zone and the Menderes Massif from north to south, respectively. The Tavşanlı zone consists of a volcano-sedimentary sequence affected by high pressure/low temperature (HP/LT) metamorphism, and this blueschist belt rests with a tectonic contact on the Afyon Zone to the south [46]. The Tavşanlı Zone was thrust over the Afyon zone, which consists of shelf-type greenschist facies metasediments of Paleozoic-Mesozoic age affected by low-grade regional metamorphism [46-49]. The Afyon Zone rests directly on the gneisses of the Menderes Massif [50]. [51] suggested that the Afyon zone of the Anatolides uncomformably overlies the Menderes Massif. [36] suggested that the north-south shortening of NW Turkey ceased at the end of the Oligocene and was replaced by N-S extension in the Late Miocene. Thus, the extensional regime formed the E-W-extending graben systems in the region ([52,53]; Fig. 1, Fig. 2). The Menderes Massif is interpreted as a "metamorphic core complex" formed through the listric faults [51,54-57] that constitute the boundary of the graben. The development of magmatic activity in western Anatolia is closely associated with the tectonic evolution of the region (24,25,29,46,53,58-60). As a result of the N-S compressional tectonic regime, calc-alkaline volcanism closely associated with the granitoids developed in the region.

The Simav Graben, trending WNW-ESE, is located at the study area (Fig. 2). The region is cut by E-W-trending faults, which are nearly parallel to the Simav graben fault. The other fault system trends N-S and cuts the former set of faults.

In the region, at the base, Precambrian Menderes Massive Metamorphics (Kalkan formation, Simav metamorphics, Sarıcasu formation, Arıkayası formation) is situated (Fig. 3). Kalkan formation and Sarıcasu formation cropped out in the study area. The Kalkan formation represented by migmatite and biotite-bearing gneiss (Fig. 3). The Sarıcasu formation consists of quartz, albite, chlorite and muscovite-bearing schists. The Budağan limestone unconformably overlies the metamorphics, starting with a conglomerate level that includes abundant quartz pebbles. These units are tectonically overlain by Upper Cretaceous Dağardı melange. As Miocene sediments (Kızılbük formation) cover to this unit, unconformably. Lower Miocene aged Akdağ volcanite cut these units. Plio-Quaternary Toklargölü formation and actual aluvvium cover to Upper Pliocene Payamtepe volcanites consist of basalts and the other all units, unconformably ([11,13,50]; Fig. 3).
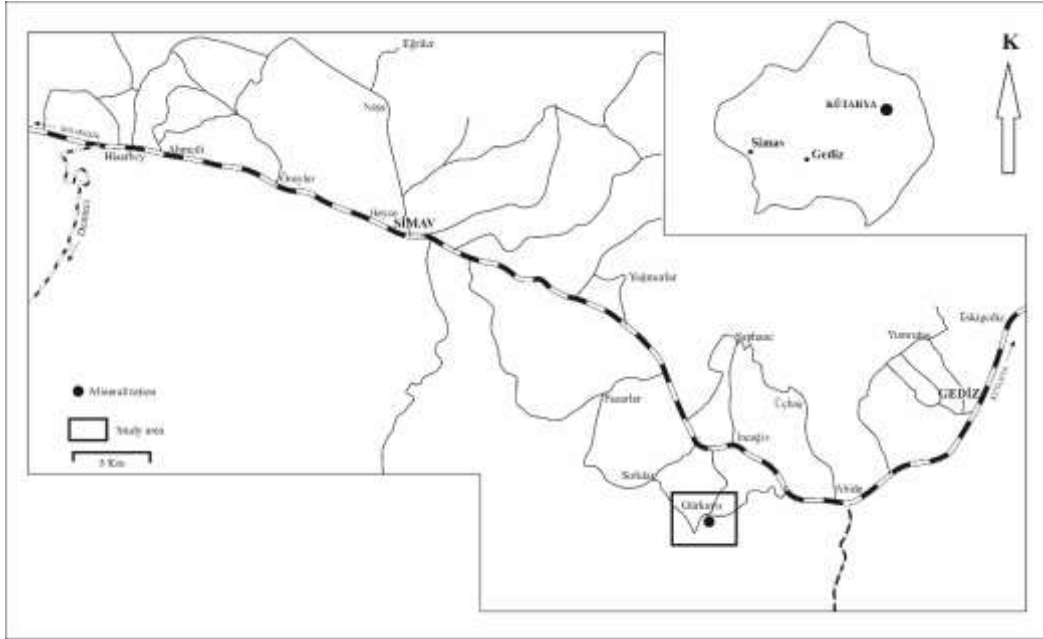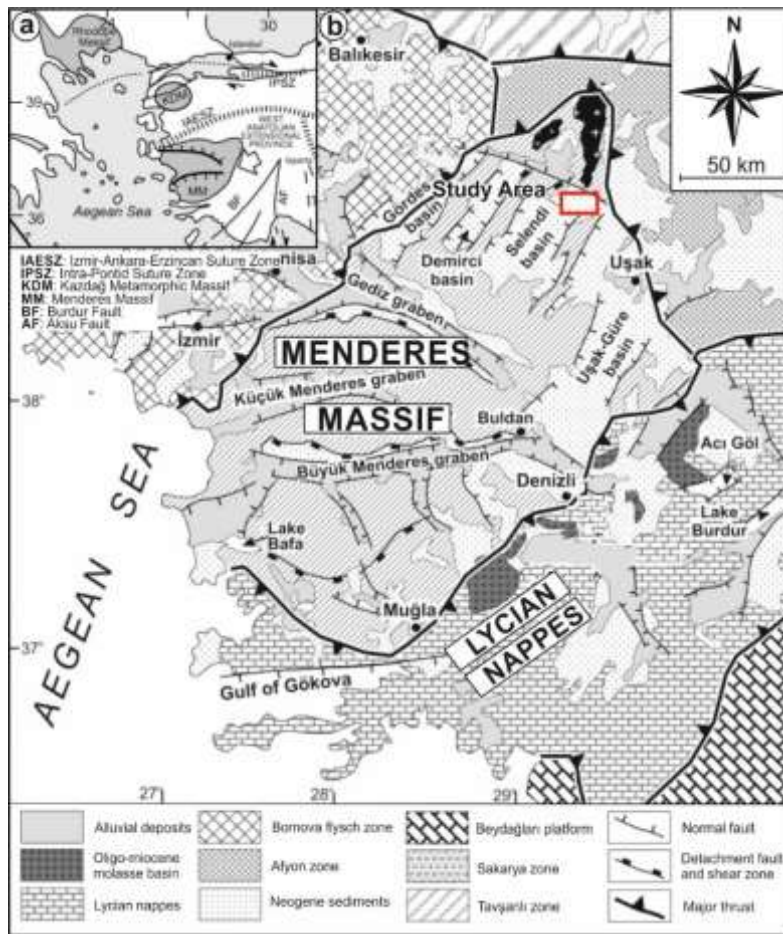
Figure 1. Location map of the Gürkuyu Sb mineralization.

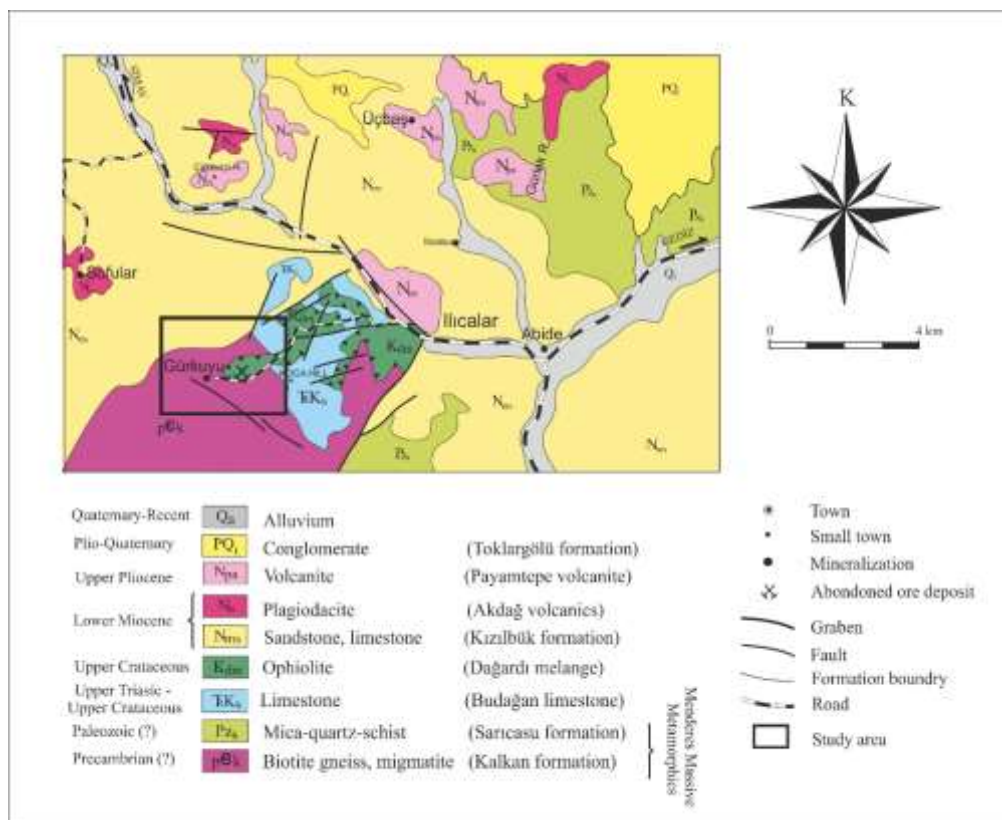**Figure 2.** Tectonical map of the Gürkuyu Sb mineralization

Figure 3. Regional geological map of the study area (modified after 11,50).

2.2. Local geological setting – Gürkuyu Sb mineralization

The Gürkuyu Sb mineralization is located at west of the Koca hill in east of Gürkuyu village of Gediz (Kütahya-Turkey). Serpentinites of Dağardı melange and crystallized limestones of Budağan limestone were hydrothermally altered by hydrothermal solutions, come from fissures and fractures due to tectonic movement during the thrust of melange and occurred silicified zone. Gürkuyu Sb mineralization suggest that occurred in this silicified zone (Fig. 4, Fig. 5).

Traces of ancient mining activities such as adit are observed at Gürkuyu Sb mineralization. This mineralization includes stibnite, pyrite, valentinite/senarmontite, orpiment and realgar. The alteration products are determined as quartz according to the XRD analysis.

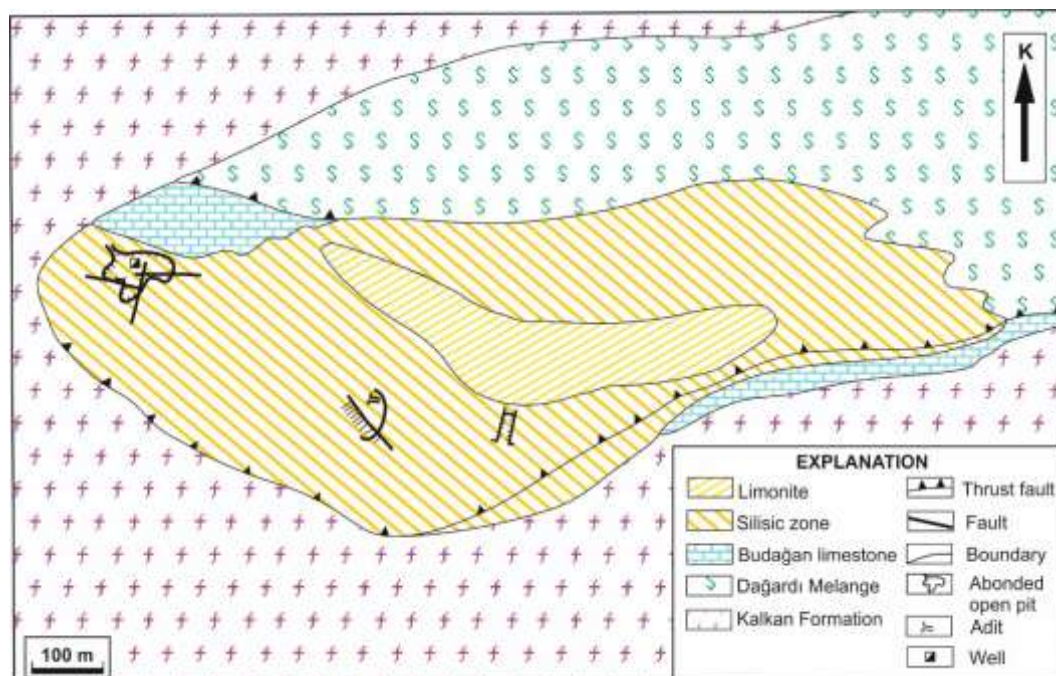**Figure 4.** Photographs from gallery of the Gürkuyu Sb mineralization

Figure 5. Local geological map of the study area (modified after [11,50]).

3. MATERIALS AND METHODS

3.1. Geochemistry

Sixteen samples were selected for whole-rock chemical analysis. The ore samples and silisic alteration samples were crushed, quartered, pulverized to 125 mesh and homogenized. Geochemical analysis was carried out to determine the bulk geochemistry of the ore samples in ACME Analytical Laboratories Ltd., Vancouver, Canada. Analyses were carried out by ICP-Emission Spectrometry for major oxides and ICP-Mass Spectrometry for trace and Rare Earth Elements (REE), following the lithium metaborate/tetraborate fusion and dilute nitric digestion. In addition, a separate 0.5 g split is digested in Aqua Regia and analyzed for ICP Mass Spectrometry for trace and rare earth elements. Detection limits are 0.01% for SiO_2, Al_2O_3, MgO, CaO, Na_2O, K_2O, TiO_2, P_2O_5 and MnO; 0.04% for Fe_2O_3; 0.02% for Cr_2O_3; 0.01 ppm for Hg, Tm, Lu; 0.5 ppm for Sr and W; 0.1 ppm for Zr, Y, La, Ce, Bi, Ta, Nb, Hf, Ag, Cd, Sb, Mo, Ni; 0.05 ppm for Sm, Gd, Dy, Yb and 8 ppm for V. Au has 0.5 ppb detection limit. Detection limits for Pr and Eu were 0.02 ppm. The detection limits for Pb were 0.1%. The detection limit was 0.001% for Cu. Detection limits were 1 ppm for Ba, Zn, Sc and Sn; 0.3 ppm for Nd and 0.03 ppm for Er.

3.2. Ore petrography

Polished sections were prepared in Geological Engineering Department of Selçuk University and ore petrography laboratory of the General Directorate of Mineral Research and Exploration (MTA, Ankara). Identification and characterization of the mineral assemblages were carried out using a Nikon LV100 Pol microscope equipped with Nikon (12MP) digital camera in Niğde University (Niğde).

3.3. Sulfur isotopes

The sulfur isotope analyses were performed on pyrite collected from mineralization in the Environmental Isotope Laboratory at the University of Arizona using an elemental analyzer (Costech) coupled to the mass spectrometer. It's an adaptation (automation) of an old technique of [61]. $\delta^{34}S$ was measured on SO_2 gas in a continuous-flow gas-ratio mass spectrometer (ThermoQuest Finnigan Delta PlusXL). Samples were combusted at 1030 °C with O_2 and V_2O_5 using an elemental analyzer (Costech) coupled to the mass spectrometer. Standardization is based on international standards OGS-1 and NBS123, and several other sulfide materials that have been compared between laboratories. Calibration is linear in the range -10 to +30 per mil. Precision is estimated to be ± 0.15 or better (1s), based on repeated internal standards.

3.4. Oxygen isotopes

The oxygen isotope analyses of quartz were performed at the Queen's Facility for Isotope Research, Queen's University, Canada, following the procedure of [62]. Approximately 5 mg of powdered sample were heated, using a conventional resistance furnace, in BrF5 atmosphere at ca. 550 °C overnight to extract oxygen, which was then converted to CO_2 by contact with a heated carbon rod. The CO_2 was analysed off-line using a Finnigan-Mat 252 isotope ratio mass spectrometer. The raw data were converted to $d^{18}O$ relative to V-SMOW by comparison with results from an in-house standard CO_2 gas analysed simultaneously. The precision of the $d^{18}O$ values are reproducible within ± 0.3 per mil, based on repeated analyses of an in-house standard.

3.5. Scanning Electron Microscopy (SEM-EDX)

Morphological and qualitative analyses of the mineralization samples were performed using SEM-EDX. The SEM provided information on the physical properties of minerals, while EDX provided information on their chemistry. SEM-EDX microanalysis and microphotographs were carried out using a ZEISS/EVO LS10 equipped with BRUKER QUANTAX 200 sensor at the Advanced Technology, Research and Application Center of Selçuk University.

3.6. X-ray diffraction (XRD)

The compositions of the clay minerals were analyzed by X-ray diffraction (XRD). The XRD analyses were carried out using Rigaku X-ray diffractometer at the XRD laboratories of the General Directorate of Mineral Research and Exploration (MTA, Ankara) and Gebze Technical University (Kocaeli).

4. RESULTS

4.1. Ore petrography, SEM-EDX and X-ray diffraction

The ore microscopic, XRD and SEM-EDX investigations reveal that the ore mineral assemblage in the Gürkuyu Sb mineralization consists of stibnite, pyrite associated with gangue quartz and accompanied by secondary ore minerals, such as senarmontite/valentinite, orpiment and realgar (Fig. 6-8). In Gürkuyu Sb mineralization, the alteration samples characterized by silisic alteration based on XRD analyses are composed mainly of quartz. The quartz observed commonly in silicification is euhedral. In the polished sections, the observed minerals are as follows stibnite and pyrite in the ore samples (Fig. 6-8).

Stibnite is the most abundant ore mineral and occurs in all polished sections. Fine grained stibnites are generally found at the euhedral. Pyrite is one of the common minerals in the mineralization. The euhedral pyrites have cataclastic structured and spongy textured. Some of the pyrites is observed as framboidal texture (Fig. 7).

Figure 6. Photographs showing macro ore minerals from the Gürkuyu Sb mineralization (a), (b), (c) and (d) photographs showing mainly antimuan okr with skeletal texture and radial antimony (e), (f) antimony, pyrite, orpiment and realgar.
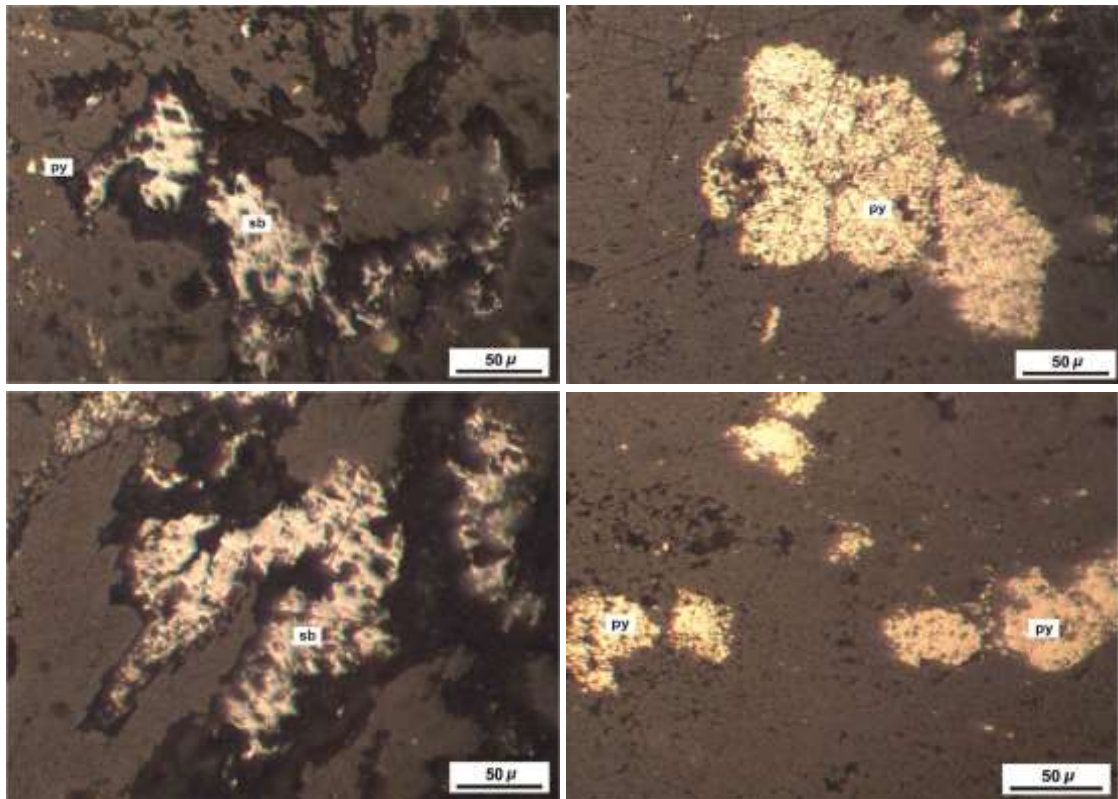
Figure 7. Photographs showing micro ore minerals from the Gürkuyu Sb mineralization (sb: stibnite/antimony, py: pyrite).
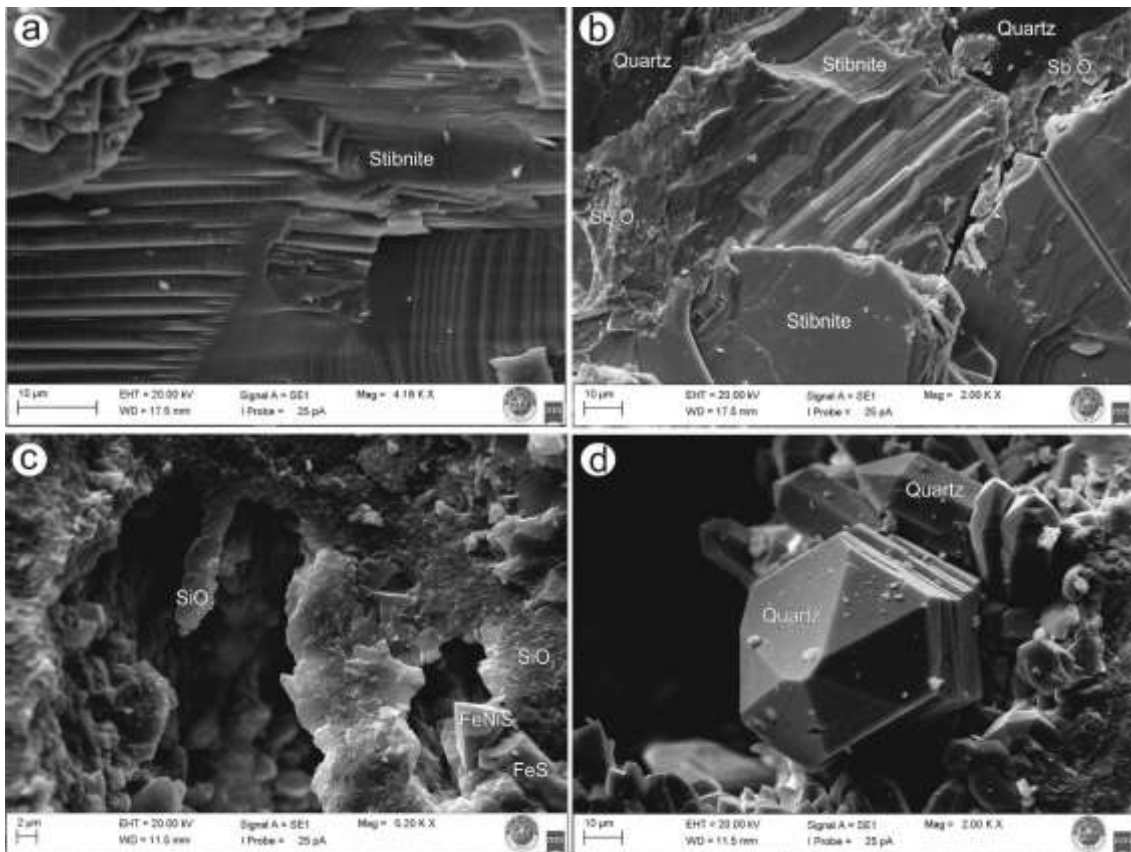

Figure 8. Scanning Electron Microscope images of the stibnite, Sb_2O_3 (valentinite/senarmontite) and quartz.

4.2. Geochemistry

Based on mineralogical and petrographical studies, a total of 11 samples (5 samples of mineralization, 6 samples of silisic alteration) were selected for major, trace and rare earth element (REE) analysis. The results of analyses are presented in Table 1.

4.2.1. Geochemistry of mineralization and silisic alteration

Contents of the major oxide, trace and REE data belonging to 11 samples from Gürkuyu Sb mineralization and silisic alteration are shown in Table 1. The average composition of the Gürkuyu Sb mineralization was determined to be Sb dominated, according to the geochemical analyses of ore samples collected from the mineralization. In mineralization, average contents of Fe_2O_3, Sb, Hg, As and Au are 2.15 wt.%, 13359 pm, 1.12 ppm, 1367 ppm and 163.82 ppb, respectively. Geochemical studies indicate that the Gürkuyu Sb mineralization is rich in Sb and As content in GU-3, reaching up to 27710 ppm and 4673 ppm, respectively (Table 1). In silisic alteration, SiO_2 and Sb values are 90.05 wt.% and 111 ppm, respectively.

Table 1. Geochemical results of the Gürkuyu Sb mineralization and silisic alteration.

Sample		Mineralization						Silisic Alteration						
		KO-13	KO-16	KO-27	GU-2	GU-3	Average	KÖ-1	KÖ-2	KÖ-3L	KÖ-5	KÖ-8C	KÖ-19	Average
SiO_2	wt.%	69.84	94.23	95.79	74.17	86.92	**84.19**	95.29	89.87	83.49	93.86	92.77	85.00	**90.05**
Al_2O_3	wt.%	0.67	1.27	0.89	0.56	0.96	**0.87**	0.94	0.17	0.28	0.48	1.62	0.53	**0.67**
Fe_2O_3	wt.%	1.32	1.74	1.74	2.45	3.50	**2.15**	1.54	6.36	12.95	2.58	2.34	9.26	**5.84**
MgO	wt.%	0.11	0.20	0.14	3.85	0.22	**0.90**	0.08	0.07	0.06	0.11	0.22	0.46	**0.17**
CaO	wt.%	0.86	0.32	0.32	5.79	0.13	**1.48**	0.05	0.06	0.05	0.21	0.27	0.44	**0.18**
Na_2O	wt.%	0.03	0.02	0.02	0.03	0.02	**0.02**	0.03	0.03	0.01	0.05	0.02	0.02	**0.03**
K_2O	wt.%	0.08	0.13	0.12	0.07	0.13	**0.11**	0.09	0.06	0.04	0.12	0.27	0.06	**0.11**
MnO	wt.%	0.02	0.05	0.05	0.05	0.03	**0.04**	0.02	0.07	0.03	0.01	0.02	0.12	**0.05**
Cr_2O_3	wt.%	0.17	0.24	0.12	0.26	0.44	**0.25**	0.27	0.28	0.20	0.32	0.33	0.33	**0.29**
Ba	ppm	308.00	70.00	151.00	118.00	38.00	**137.00**	182.0	97.00	44.00	138.0	30.00	373.0	**144.0**
Co	ppm	64.50	29.10	13.90	52.60	75.70	**47.16**	7.70	26.80	27.50	7.00	43.30	160.3	**45.43**
Nb	ppm	0.50	0.50	0.40	0.20	0.10	**0.34**	0.60	0.30	0.30	0.20	0.10	0.30	**0.30**
Rb	ppm	5.20	10.30	8.20	5.00	11.00	**7.94**	4.30	0.60	1.80	6.90	17.30	5.10	**6.00**
Sr	ppm	92.40	23.80	40.80	91.60	15.70	**52.86**	38.00	5.70	7.60	142.8	29.00	25.20	**41.38**
V	ppm	37.00	26.00	13.00	17.00	36.00	**25.80**	25.00	60.00	137.0	28.00	60.00	123.0	**72.17**
Zr	ppm	0.90	2.70	1.90	2.90	3.00	**2.28**	4.20	2.50	2.10	0.50	1.80	2.90	**2.33**
Mo	ppm	0.10	0.70	0.80	0.30	1.20	**0.62**	0.80	0.70	4.80	0.50	0.30	1.20	**1.38**
Cu	ppm	0.10	5.90	6.80	4.60	20.40	**7.56**	10.30	7.30	5.90	4.70	8.90	15.20	**8.72**

Pb	ppm	0.20	4.50	6.90	89.90	7.80	**21.86**	12.20	0.80	2.00	6.50	22.80	11.80	**9.35**
Zn	ppm	6.00	16.00	34.00	189.00	11.00	**51.20**	5.00	23.00	22.00	6.00	12.00	33.00	**16.83**
Ni	ppm	836.25	240.30	155.15	945.40	1100.40	**655.50**	99.95	837.65	667.2	69.70	398.4	2885	**826.3**
As	ppm	14.80	660.50	769.50	716.80	4673.80	**1367.08**	190.27	36.20	637.2	2200	3360	2362	**1581**
Sb	ppm	14987.0	1021.7	1478.02	1600.0	21600.0	27710.0	**13359.34**	77.40	87.40	24.80	162.7	267.5	46.10	**111.0**
Ag	ppm	1.70	0.10	0.40	0.70	1.70	**0.92**	0.10	0.10	0.10	0.20	0.10	0.10	**0.12**
Au	ppb	14.80	3.60	27.10	10.10	763.50	**163.82**	1.30	4.60	3.30	6.20	24.20	37.30	**12.82**
Hg	ppm	0.15	0.88	1.22	0.52	2.81	**1.12**	0.10	0.03	1.83	1.77	0.82	1.06	**0.94**
Y	ppm	0.40	0.70	0.30	0.20	0.10	**0.34**	0.50	1.80	1.40	0.10	0.40	0.80	**0.83**
Sc	ppm	1.00	3.00	2.00	3.00	2.00	**2.20**	1.00	3.00	1.00	3.00	3.00	8.00	**3.17**
La	ppm	8.20	1.60	0.50	1.70	1.70	**2.74**	1.60	1.10	0.90	0.20	0.40	0.60	**0.80**
Ce	ppm	0.90	1.90	0.40	0.30	0.30	**0.76**	2.80	1.40	2.00	0.40	0.40	0.70	**1.28**
Pr	ppm	0.10	0.31	0.06	0.04	0.03	**0.11**	0.37	0.27	0.24	0.08	0.05	0.12	**0.19**
Nd	ppm	0.30	1.10	0.30	0.30	0.30	**0.46**	1.20	1.00	0.80	0.30	0.50	0.40	**0.70**
Sm	ppm	0.07	0.24	0.06	0.05	0.05	**0.09**	0.25	0.22	0.21	0.07	0.06	0.16	**0.16**
Eu	ppm	0.02	0.04	0.02	0.02	0.02	**0.02**	0.06	0.05	0.05	0.02	0.03	0.04	**0.04**
Gd	ppm	0.05	0.18	0.05	0.05	0.05	**0.08**	0.19	0.23	0.21	0.05	0.09	0.13	**0.15**
Tb	ppm	0.02	0.02	0.01	0.01	0.01	**0.01**	0.04	0.05	0.03	0.01	0.01	0.03	**0.03**
Dy	ppm	0.12	0.16	0.05	0.05	0.05	**0.09**	0.15	0.24	0.20	0.05	0.05	0.11	**0.13**
Ho	ppm	0.02	0.03	0.02	0.02	0.02	**0.02**	0.04	0.07	0.05	0.02	0.02	0.02	**0.04**
Er	ppm	0.03	0.07	0.03	0.03	0.03	**0.04**	0.07	0.17	0.11	0.03	0.09	0.09	**0.09**
Tm	ppm	0.02	0.01	0.01	0.01	0.01	**0.01**	0.03	0.03	0.02	0.01	0.02	0.02	**0.02**
Yb	ppm	0.06	0.06	0.05	0.05	0.05	**0.05**	0.05	0.20	0.11	0.05	0.05	0.05	**0.09**
Lu	ppm	0.01	0.01	0.01	0.01	0.01	**0.01**	0.03	0.04	0.02	0.01	0.01	0.02	**0.02**
LOI	wt.%	7.40	1.70	0.70	9.20	3.80	**4.56**	1.50	2.80	2.40	2.20	2.00	3.30	**2.37**
Total	wt.%	80.50	99.90	99.89	96.43	96.15	**94.57**	99.97	99.98	99.98	99.96	99.98	99.93	**99.97**
∑REE(La-Lu)		9.92	5.73	1.57	2.64	2.63	**4.50**	6.88	5.07	4.95	1.30	1.78	2.49	**3.75**
∑LREE(La-Sm)		9.57	5.15	1.32	2.39	2.38	**4.16**	6.22	3.99	4.15	1.05	1.41	1.98	**3.13**
∑HREE(Gd-Lu)		0.33	0.54	0.23	0.23	0.23	**0.31**	0.60	1.03	0.75	0.23	0.34	0.47	**0.57**

4.3. Stable isotopes

4.3.1. S isotopes

4.3.1.1. Sulfur isotope composition of pyrite

In Gürkuyu Sb mineralization, $\delta^{34}S$ values of stibnite are ranged from 1.0 ‰ to 1.3 ‰ (Table 2, Figure 9). The $\delta^{34}S$ values of stibnite display a narrow range. So, the source of the sulfur during the formation of these minerals can be considered a sign that it has a homogeneous isotopic composition [63]. Therefore, it is consistent with the sulfur in stibnite is derived from the only one phase in Gürkuyu Sb mineralization.

Table 2. Sulfur isotope ($\delta^{34}S$) values for stibnite of the Gürkuyu Sb mineralization.

Sample No	$\delta^{34}S$ (‰) values of stibnite
GÜ-3-1	1.3
GÜ-3-2	1.0
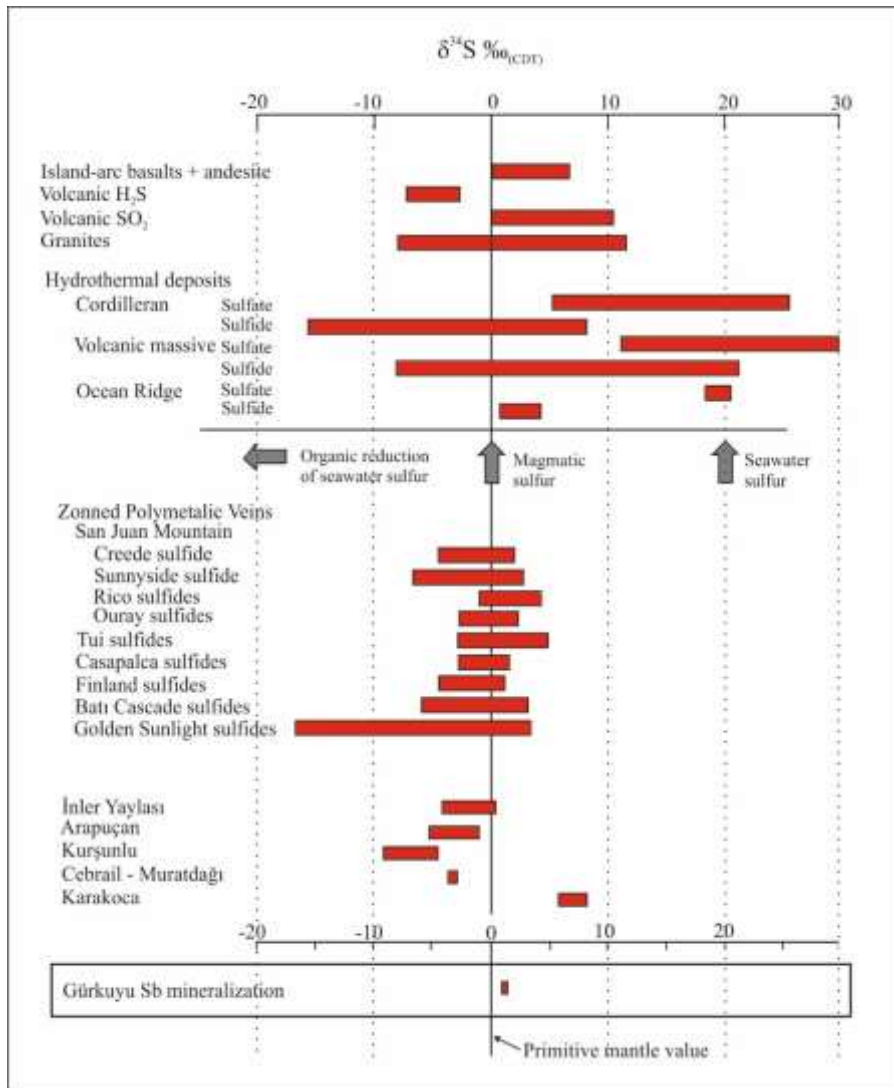
Figure 9. Comparison of the Gürkuyu Sb mineralization, natural sulfur isotope reservoirs and mineralizations from the Turkey and globally. (Natural sulfur isotope reservoirs [64]; (global mineralizations, [65]; mineralizations from the Turkey, [63,66-69].

4.3.2. O isotopes

4.3.2.1. Oxygen isotope compositions of quartz

The $\delta^{18}O$ value of quartz is 15.8 ‰ in Gürkuyu Sb mineralization (Table 3). Sulfur and oxygen isotope values are similar to the values for magmatic rocks and to the values for fluids of magmatic origin (Fig. 10).

Table 3. Oxygen isotope ($\delta^{18}O$) values for quartz of the Gürkuyu Sb mineralization.
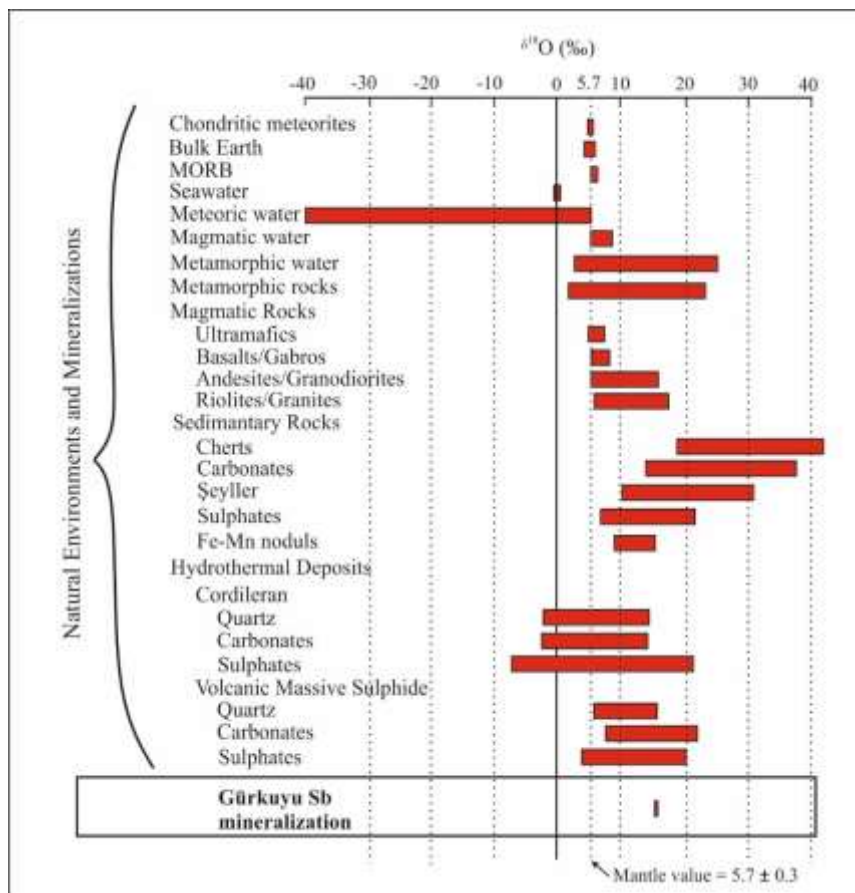
Sample No	$\delta^{18}O$ (‰) values of quartz
GÜ-3	15.8

Figure 10. Arpaçukuru Fe-Cu mineralization comparison with other natural oxygen isotope reservoirs and mineralizations (modified after [65]).

5.   DISCUSSION

The hydrothermal base-metal (Cu-Pb-Zn) veins are located at the northern block of the Simav Graben [68,70-73]. These mineralizations occur in the granitoids and gneisses. The Gürkuyu Sb mineralization, located in the gneiss and melange, in the southern block of the Simav Graben.

The Menderes Massif hosts a variety of hydrothermal mineral deposits, including gold, copper, antimony, uranium and mercury. While there is evidence for gold mineralization during crustal

shortening, most other deposit types including epithermal gold, detachment gold, mercury, and sandstone-hosted uranium formed during the Miocene to recent crustal extension [74].

Both the Menderes core complex and the Eastern Rhodopes in Bulgaria exhibit exhumation histories of surprisingly similar duration (approximately 35–45 Ma) and similar evolution of mafic magmatism. Similar mechanisms likely explain these processes in the two regions [75]. The Rhodope Massif, like the Menderes Massif, is characterized by numerous small to moderate-sized polymetallic ore deposits of variable composition and ore type, some of which are grouped into ore districts of global significance [76-78].

6. CONCLUSIONS

The Gürkuyu Sb mineralization is mineralized with stibnite, pyrite, quartz and accompanied by minor amounts of senarmontite/valentinite, orpiment and realgar.

The mineralogy of the mineralization, the dominance of the Sb associations, plus the stable isotopes, indicate that the Gürkuyu mineralization system is a low-temperature hydrothermal mineralization.

Serpentinites and crystallized limestones were hydrothermally altered by hydrothermal solutions, come from fissures and fractures due to tectonic movement during the thrust of melange and occurred silicified zone. Gürkuyu Sb mineralization suggest that occurred in this silicified zone.

The $\delta^{34}S$ composition of the mineralization indicates a magmatic signature. Narrow sulfur isotope data indicate that the Gürkuyu Sb mineralization derived from a single magmatic hydrothermal system.

Oxygen isotope value obtained on quartz is similar to a magmatic environment. These data suggest the presence of a magmatic-hydrothermal solution.

The field observation, stable isotope data, chemical, macroscopic and microscopic data in Gürkuyu Sb mineralization suggest the presence of a low-temperatured hydrothermal (epithermal) solution.

REFERENCES

1. Janković S. (1997) The Carpatho–Balkanides and adjacent area: a sector of the Tethyan Eurasian metallogenic belt, Miner Deposita 32, 426–433.
2. Power-Fardy D., Magaranov G. (2013) A technical review of the Borsko Jezero copper- gold property, Bor, Serbia for Mundoro Capital Inc., Watts, Griffis and McOuat Limited,Toronto, Canada, 74 pp.
3. Kuşcu İ., Gençalioğlu-Kuşcu G., Tosdal R., Ulrich T., Friedman R. (2011) The geochronology of gold–copper deposition and temporal association with magmatic rocks in western Anatolia. 64th Geological Congress of Turkey, April 25–29, Abstracts, Ankara.
4. Kuşcu İ. (2009) Metallogenesis of the Tethyan Collage: Magmatic association and age of ore deposition in Turkey, MDRU Industry collaborative initiative, Project report: Update to sponsor companies, MDRU contribution No. 269, 38p.

5. Aldanmaz E., Pearce J.A., Thirlwall M.F., Mitchell J.G. (2000) Petrogenetic evolution of late Cenozoic, post-collision volcanism in western Anatolia, Turkey: Journal of Volcanology and Geothermal Research, v. 102, p. 67 - 95.

6. Doglioni C., Agostini S., Crespi M., Innocenti F., Manetti P., Riguzzi F., Savaşçın Y. (2002) On the extension in western Anatolia and the Aegean Sea, in Rosenbaum, G., and Lister, G.S., eds., Reconstruction of the evolution of the Alpine-Himalayan Orogen: Journal of the Virtual Explorer, 8, 169–183.

7. Kuşcu İ., Tosdal, R.M., Gencalioğlu - Kuşcu, G. (2013b) Metallogenesis of Turkish Tethyan collage: Characteristics, Tectonic Setting, Petrogenesis and Geochronology of Porphyry deposits and Associated Magmatism in Turkey, Economic Geology.

8. van Hinsbergen D, Kaymakcı N., Spakman W., and Torsvik T.H. (2010) Reconciling the geological history of western Turkey with plate circuits and mantle tomography, Earth and Planetary Science Letters, v. 297, p. 674 – 686.

9. Yiğit Ö. (2009) Mineral deposits of Turkey in relation to Tethyan Metallogeny: implications for future mineral exploration. Econ. Geol. 104, 19–51.

10. Yiğit Ö. (2012) A prospective sector in the Tethyan Metallogenic Belt: Geology and geochronology of mineral deposits in the Biga Peninsula, NW Turkey, Ore Geology Reviews, 46, 118-148.

11. Özen Y. (2012) Genetic Modelling of the Polymetalic Mineralizations between Ahmetli (Simav-Kütahya) – Pınarbaşı (Gediz-Kütahya). PhD thesis, Selçuk University, Turkey, 302 p.

12. Özen Y., Arık F. (2013a) Fluid Inclusion and Sulfur Isotope Thermometry in the İnkaya (Simav-Kütahya) Cu-Pb-Zn-(Ag) Mineralization, NW Turkey, ECROFI XXII, Antalya, 4-9 June, 167-168.

13. Özen Y., Arık, F. (2013b) Fluid inclusion and sulfur isotope thermometry of the İnkaya (Simav-Kütahya) Cu-Pb-Zn-(Ag) Mineralization, NW TURKEY, Cent. Eur. J. Geosci., 5(3), 435-449.

14. Özen Y., Arık F. (2015) S, O and Pb isotopic evidence on the origin of the İnkaya (Simav-Kütahya) Cu–Pb–Zn–(Ag) Prospect, NW Turkey, Ore Geology Reviews, 70, 262–280.

15. Özen, Y., Arık, F., 2016. "Genetic relationship of polymetallic hydrothermal Değirmenciler Sb, İnkaya Cu-Pb-Zn-(Ag) and Arpaçukuru Fe-Cu mineralizations in Simav (Kütahya-NW Turkey)", 1st International Underground Resources and Energy Conference, Yozgat, 68.

16. Özen, Y., Arık, F., 2016. "Geochemical, Fluid Inclusion and Isotopic (S, O, Pb) Investigations of Pınarbaşı Pb-Zn Mineralization (Gediz-KÜTAHYA) NW Turkey", 1st International Underground Resources and Energy Conference, Yozgat, 67.

17. Özen, Y., Arık, F., 2016. Stable isotope investigation of Gürkuyu Sb mineralization (Gediz-Kütahya-NW Turkey), 1st International Underground Resources and Energy Conference, Yozgat, 99.

18. Arık, F. and Özen, Y., 2016. Mineralogical, Geochemical and Sulfur Isotopic Constraints on the Origin of the Arpaçukuru Fe-Cu Mineralization (Simav-KÜTAHYA) NW Turkey, ICONSETE-2, Barcelona, Spain.

19. Erkül F., Erkül Tatar S. (2010) Geology of the Early Miocene Alaçamdağ (Dursunbey-Balikesir) magmatic complex and implications for the Western Anatolian extensional tectonics, Mineral Res. Expl. Bull., 141, 1-25.

20. Altunkaynak S., Yılmaz Y. (1998) The Mount Kozak magmatic complex, western Anatolia, J. Volcanol. Geothermal Res. 85, 211–231.

21. Karacık Z., Yılmaz Y. (1998) Geology of the ignimbrites and the associated volcano–plutonic complex of the Ezine area, northwestern Anatolia, Journal of Volcanology and Geothermal Research 85, 251–264.

22. Westaway R. (2006) Cenozoic cooling histories in the Menderes Massif western Turkey, may be caused by erosion and flat subduction, not low-angle normal faulting. Tectonophysics, 412 1-2, 1-25.

23. Hasözbek A., Satır M., Erdoğan B., Akay E., Siebel W. (2009) U-Pb Geochronology and Sr-Nd Isotopic Composition of Collision Related Granites in NW Anatolia: Contrasting Petrogenetic Evolution of the Magmatic Suites. 62nd Geological Kurultai of Turkey, 13−17 April 2009, General Directorate of Mineral Research and Exploration, Ankara, Turkey, 490-491.

24. Altunkaynak Ş., Dilek Y. (2006) Timing and nature of postcollisional volcanism in western Anatolia and geodynamic implications, In: Dilek, Y., and Pavlides, S., (Eds.), Postcollisional tectonics and magmatism in the Mediterranean region and Asia: Geological Society of America Special Paper, 409, 321 – 351.

25. Işık V., Gürsu S., Göncüoğlu C., Seyitoğlu G. (2004) Deformational and geochemical features of syn-tectonic Koyunoba and Egrigöz granitoids, western Turkey. In 5 th International Symposium on Eastern Mediterranean Geology, Thessaloniki, Greece, 3, 1143-1146.

26. Delaloye M., Bingöl E. (2000) Granitoids from Western and Northwestern Anatolia. Geochemistry and Modeling of Geodynamic Evolution, International Geology Review, 42, 241-268.

27. Seyitoğlu G. (1997) The Simav graben: an example of young E-W trending structures in the late Cenozoic extensional system of western Turkey, Turkish J. Earth Sci., TÜBİTAK, 6, 135-141.

28. Seyitoğlu G., Scott B.C. (1992) Late Cenozoic volcanic evolution of the northeastern Aegean region, Journal of Volcanology and Geothermal Research, 54, 157-176.

29. Savaşçın M.Y., Güleç N. (1990) The relationship between magmatic and tectonic activities in western Turkey. In: M.Y. Savaşçın, H. Eronat (Editors) IESCA-90, Proceedings, 2, 300-313.

30. Bozkurt E. (2001) Neotectonics of Turkey-a synthesis, Geodinamica Acta, 14, 3–30.

31. Şengör A.M.C., Yılmaz Y. (1981) Tethyan Evolution of Turkey: A Plate Tectonic Approach. Tectonophysics, 75, 181-241.

32. Koçyiğit A., Yusufoğlu H., Bozkurt E. (1999) Evidence from the Gediz graben for episodic two-stage extension in western Turkey. Journal of the Geological Society, 156, 605-616.

33. Altunkaynak Ş. (2007) "Collision-driven slab breakoff magmatism in northwestern Anatolia, Turkey", Journal of Geology, 115, 63-82.

34. Ring U., Gessner K., Güngör T., Passchier C.W. (1999) The Menderes massif of western Turkey and the Cycladic massif in the Ae-gean-do they really correlate? J. Geol. Soc. London, 156, 3-6.

35. Lister G.S., Bunga G., Feenstra, A. (1984) Metamorphic core complexes of Cordilleran type in the Cyclades, Aegean Sea, Greece, Geology, v. 12, p. 221-225.

36. Seyitoğlu G., Scott, B. C. (1991) Late Cenozoic crustal extension and basin formation in west Turkey. Geological Magazine, 128, 155-166.

37. Seyitoğlu G., Scott B.C., Rundle C.C. (1992) Timing of Cenozoic extensional tectonics in west Turkey, Journal of the Geological Society, London, 149, 533-38.

38. Ring U., Gessner K., Güngör T., Passchier C.W. (1999) The Menderes massif of western Turkey and the Cycladic massif in the Ae-gean-do they really correlate? J. Geol. Soc. London, 156, 3-6.

39. Doglioni C., Agostini S., Crespi M., Innocenti F., Manetti P., Riguzzi F., Savasçın Y. (2002) On the extension in western Anatolia and the Aegean Sea, in Rosenbaum, G., and Lister, G.S., eds., Reconstruction of the evolution of the Alpine-Himalayan Orogen: Journal of the Virtual Explorer, 8, 169–183.

40. Hetzel R., Passchier C.W., Ring U., Dora O.O. (1995a) Bivergent Extension in Orogenic Belts: the Menderes Massif (Southwestern Turkey). Geology, 23 (5), 455-458.

41. Hetzel R., Ring U., Akal C., Troesch M. (1995b) Miocene NNE-directed extensional unroofing in the Menderes Massif, southwestern Turkey. Journal of the Geological Society London, 152, 639-654.

42. Yiğit Ö., (2006) Gold in Turkey—a missing link in Tethyan metallogeny. Ore Geol. Rev. 28, 147–179.

43. Brinkmann R. (1976) Geology of Turkey. Elsevier, New York. 158 pp.

44. Şengör A.M.C. (1979) The North Anatolian transform fault: its age, offset and tectonic significance, Jour. Geol. Soc. Lond., 136, 269-282.

45. Kibici Y., İlbeyli N., Yıldız A., Bağcı M. (2010) Geochemical Constraints on the Genesis of the Sarıcakaya Intrusive Rocks, Turkey: Late Paleozoic Crustal Melting in the Central Sakarya Zone, Chemie der Erde-Geochemistry, 70, 243-256.

46. Okay A.I. (1984) Distribution and characteristics of the northwest Turkish blueschists. The Geological Evolution of the Eastern Mediterranean (ed. J.E. Dixon ve A.H.F. Robertson), Geological Society Special Publication, 17, 455-466.

47. Konak N. (1982) Geology of the Simav, PhD thesis, İstanbul University, Turkey, 179 pp.

48. Akdeniz N., Konak N. (1979a) The rock units of the Simav region of Menderes Massive and the situation of metabazic and metaultramafic rocks. Bulletin of the Geological Society of Turkey, 22, 175-184.

49. Kaya O. (1972) The main lines of the ophiolite problem in Tavşanlı region, Bulletin of the Geological Society of Turkey, 15, 1, 26-108.

50. Oygür V. (1997) Metallogeny of the Simav graben (Inner Western Anatolia, Turkey). PhD thesis, Middle East Technical University (METU), Ankara, Turkey, 144 pp.

51. Şengör A.M.C., Satır M., Akkök R. (1984) Timing of tectonic events in the Menderes Masif western Turkey: implications for tectonic evolution and evidence for Pan-African basement in Turkey. Tectonics, (3), 693-707.

52. Şengör A.M.C., Görür N., Saroğlu F. (1985) Strike slip faulting and related basin formation in zones of tectonic escape: Turkey as a case study. In: Biddle, T.R., Christic-Blick, N. (Eds.), Strike-slip Deformation, Basin Formation and Sedimentation. Soc. Econ. Paleontol. Min. Spec. Publ., 37, 227-264.

53. Dora Ö.O., Kun N. Candan, O. (1990) Metamorphic history and geotectonic evolution of the Menderes massif. I.E.S.C.A., 2, 102-115.

54. Bozkurt E., Park R.G. (1994) Southern Menderes Massive: an incipient metamorphic core complex in western Anatolia, Turkey. J Geol. Soc. London, 151, 213-216.

55. Shelton J.W. (1984) Listric normal faults: an illustrated summary. American Association of Petroleum Geologists Bulletin, 68, 801-815.

56. Lister G.S., Davis G.A. (1989) The origin of metamorphic core complexes and detachment faults formed during tertiary continental extension in the northern Colorado River region. U.S.A. Journal of Structural Geology, 11, 65-94.

57. Doğan A., Emre Ö. (2006) Northern boundary of the Aegean graben system: Sındırgı-Sincanlı fault zone. 59th Geological Congress of Turkey, 83-84.

58. Bingöl E., Delaloye M. and Ataman G. (1982) Granitic intrusions in western Anatolia: a contribution to the geodynamic study of this area. Eclogea Geologica Helvetica, 75, 437-446.

59. Işık V. (2004) Micro-tectonic Features of Simav Shear Zone, Northern Menderes Massive, Western Turkey. Bulletin of the Geological Society of Turkey, 47/2, 49-91.

60. Akay E. (2008) Geology and petrology of the Simav Magmatic Complex (NW Anatolia) and its comparison with the Oligo-Miocene granitoids in NW Anatolia: implications on Tertiary tectonic evolution of the region. Int J Earth Sci, 98(7), 1655-1675.

61. Coleman M. L., Moore, M.P. (1978) Direct reduction of sulfates to sulfur dioxide for isotopic analysis. Anal. Chem., 50, 1594-1598.

62. Clayton R.N., Mayeda T.K. (1963) The use of bromine pentafluoride in the extraction of oxygen from oxides and silicates for isotopic analysis, Geochim. Cosmochim. Acta, 27, 43-52.

63. Gökçe A. (1990) Sulfur isotope investigation in Kurşunlu (Ortakent-Koyullusar-SİVAS) Pb-Zn-Cu deposits, M. T. A. Bulletin, 111, 111-118.

64. Field C. W., Fifarek R.H. (1985) Light stable isotope systematics in the epithermal environment. In: Berger, B.R. & Bethke, P.M. (eds). Geology and geochemistry of epithermal systems. El Paso, Texas, Society of Economic Geologists, Reviews in Economic Geology, 99-128.

65. Rollinson H.R. (1993) Using Geochemical Data: Evaluation, Presentation, Interpretation, Longman, UK. 352 pp.

66. Gökçe A., Bozkaya, G. (2006) Lead and sulfur isotope evidence for the origin of the İnler Yaylası lead-zinc deposits, Northern Turkey, Journal of Asian Earth Sciences, 26, 91-97.

67. Gökçe A., Spiro B. (1994) Sulfur-isotope characteristics of the volcanogenic Cu-Zn-Pb Queensland, Australian journal of earth sciences, 41(3), pp. 255.

68. Erler A. (1979) Study of sulfur isotopes of Karakoca (Simav - Kütahya) lead-zinc deposit. Bulletin of the Geological Society of Turkey, 22, 117-119.

69. Örgün Y., Altınsoy N., Gültekin A.H., Karahan G., Çelebi N. (2005a) Natural Radioactivity Levels in Granitic Plutons and Groundwaters in Southeast Part of Eskişehir, Turkey, Applied Radiation and Isotopes, 63, 267-275.

70. Oygür V., Erler, A. (2000) Metallogeny of the Simav graben. Bulletin of the Geological Society of Turkey, 43(1), 7-19.

71. Aydın B. (2007) Genesis of polymetallic vein-type mineralization of Karakoca area Koyunoba Pluton (Simav-Kütahya). M.Sc. Thesis, Dokuz Eylül University, İzmir, 50 p.

72. Dora Ö.O. (1965) Karakoca lead mine and its geological survey. Bulletin of General Directorate of Mineral Research and Exploration, Rep. no. 3855.

73. Gümüş A. (1964) Important lead-zinc deposits of Turkey: Symposium on Mining Geology and the Base Metals, CENTO, Ankara, 155-168.

74. Gessner K., Porwal A., Markwitz V., Wedin F. (2010) Tectonic framework of hydrothermal and geothermal systems in the Menderes Massif, western Turkey. Geophysical Research Abstracts Vol. 12, EGU2010-5118-2.

75. Marchev P., Raicheva R., Downes H., Vaselli O., Chiaradia M., Moritz R. (2004) Compositional diversity of Eocene–Oligocene basaltic magmatism in the Eastern Rhodopes, SE Bulgaria: implications for genesis and tectonic setting. Tectonophysics, 393, 301– 328.

76. Stoyanov R. (1979) Metallogeny of the Rhodope Central Massif. Nedra, Moscow, 180.

77. Mitchell A.H.G., Carlie J.C. (1994) Mineralization, antiforms and crustal extension in andesitic arcs. Geological Magazine, 131, 231– 242.

78. Mitchell A.H.G. (1996) Distribution and genesis of some epizonal Zn–Pb and Au provinces in the Carpathian–Balkan region. Transactions of the Institution of Mining and Metallurgy (Section B, Applied Earth Science), 105, 127–138.